NASA TM X-216

TECHNICAL MEMORANDUM
X-216

AN EXPLORATORY INVESTIGATION OF A TRANSPORT CONFIGURATION DESIGNED FOR SUPERSONIC CRUISE FLIGHT NEAR A MACH NUMBER OF 3

By Ausley B. Carraway, Donald T. Gregory, and Melvin M. Carmel

Langley Research Center
Langley Field, Va.

NATIONAL AERONAUTICS AND SPACE ADMINISTRATION
WASHINGTON
March 1960

1P

NATIONAL AERONAUTICS AND SPACE ADMINISTRATION

TECHNICAL MEMORANDUM X-216

AN EXPLORATORY INVESTIGATION OF A TRANSPORT CONFIGURATION DESIGNED FOR SUPERSONIC CRUISE FLIGHT NEAR A MACH NUMBER OF 3*

By Ausley B. Carraway, Donald T. Gregory, and Melvin M. Carmel

SUMMARY

Results have been obtained from an investigation in the Langley Unitary Plan wind tunnel at Mach numbers from 2.3 to 4.5 of a proposed canard-type transport configuration designed for efficient cruise flight at a Mach number of 3. Tests were performed over an angle-of-attack range from about -4° to 12° and at angles of sideslip near 0° and 4°.

The results indicate that the configuration had a maximum lift-drag ratio of approximately 5.7 at a Mach number near 3 and at a Reynolds number of 3×10^6 based on the wing mean aerodynamic chord. An experimental trimmed lift-drag ratio approaching 6 is deemed possible through further refinements to the configuration. On a basis of aerodynamic efficiency, this proposed Mach number 3 transport would be economically feasible since the lift-drag ratios will approach and probably exceed 7 at full-scale flight conditions if full-scale surface conditions are compatible with model surface conditions.

INTRODUCTION

Aerodynamic technology is approaching the state in which a supersonic-cruise transport in the commercial and military field is seen to be feasible. (See refs. 1 and 2.) Such a vehicle would be of use for long-range conveyance of passengers or various military needs, such as rapid deployment of troops and equipment. The aerodynamic efficiency (lift-drag ratio) of such a configuration would be one of the prime factors influencing the realization of this type of vehicle. Recent design studies have indicated

*Title, Unclassified.

that a lift-drag ratio (L/D) of approximately 7 (for long-range aircraft) is needed in order that a Mach number 3 airliner may be made economically feasible.

Although experimental data exist on several high L/D configurations (ref. 3), these configurations, because of volume considerations, are not believed appropriate for transports; therefore, the staff of the Langley Unitary Plan wind tunnel has investigated a model of a proposed configuration for efficient cruise flight at a Mach number of 3. The configuration is of the canard type and employs a clipped-delta wing plan form with a maximum thickness ratio of $2\frac{1}{2}$ percent. The engine arrangement is designed for four engines placed side by side in a package below the wing and two engines contained in the rearward portion of the fuselage. The fuselage generally has circular sides with a flat top and is designed to carry nearly 200 passengers.

Tests were performed through an angle-of-attack range from approximately -4° to 12° at sideslip angles of approximately 0° and 4° and through a Mach number range from 2.3 to 4.5. The tests were conducted at a Reynolds number of 3×10^6 based on the mean aerodynamic chord of the wing.

SYMBOLS

The aerodynamic forces and moments are referred to the stability axes system for the longitudinal data and to the body axes system for the lateral data with the origin at the center of gravity. (See figs. 1 and 2.) The symbols used are defined as follows:

b	wing span, in.
$\bar{c}$	mean aerodynamic chord of wing, in.
C_A	axial-force coefficient, $\frac{\text{Axial force}}{qS_w}$
C_D'	drag coefficient, $\frac{\text{Drag}}{qS_w}$
$C_{D,c}'$	chamber drag coefficient, $\frac{\text{Chamber drag}}{qS_w}$
$C_{D,i}'$	internal drag coefficient, $\frac{\text{Internal drag}}{qS_w}$

$C_{D_{min}}$ minimum drag coefficient

C_L lift coefficient, $\frac{\text{Lift}}{qS_w}$

C_{L_o} lift coefficient at an angle of attack of 0^o

$C_{L_\alpha} = \frac{\partial C_L}{\partial \alpha}$ per degree

$\frac{1}{57.3 C_{L_\alpha}}$ theoretical drag due to lift of a flat plate

C_l rolling-moment coefficient, $\frac{\text{Rolling moment}}{qS_w b}$

C_m pitching-moment coefficient, $\frac{\text{Pitching moment}}{qS_w \bar{c}}$

C_{m_o} pitching-moment coefficient at $C_L = 0$

$C_{m_{C_L}} = \frac{\partial C_m}{\partial C_L}$

$C_{m_{\delta_c}} = \frac{\Delta C_m}{\Delta \delta_c}$ per degree

$C_{m_{\delta_N}} = \frac{\Delta C_m}{\Delta \delta_N}$ per degree

C_n yawing-moment coefficient, $\frac{\text{Yawing moment}}{qS_w b}$

C_Y side-force coefficient, $\frac{\text{Side force}}{qS_w}$

$\frac{dC_D}{dC_L^2}$ drag due to lift parameter

h altitude, ft

$(L/D)_{max}$ maximum lift-drag ratio

M free-stream Mach nu[redacted]

$\frac{\sqrt{M^2 - 1}}{4}$	theoretical drag due to lift of a triangular wing (supersonic leading edge)
q	free-stream dynamic pressure, lb/sq ft
R	Reynolds number; radius
S_w	wing area, sq ft
W	gross airplane weight, lb
α	angle of attack of wing chord line, deg
β	angle of sideslip of fuselage center line, deg
δ_c	canard angle, measured with respect to wing chord line (positive direction, leading edge up), deg
δ_n	nose angle measured with respect to wing chord line (positive direction, nose up), deg

APPARATUS AND TESTS

Tunnel

Tests were conducted in the high Mach number test section of the Langley Unitary Plan wind tunnel, which is a variable-pressure, continuous-flow tunnel. The nozzle leading to the test section is of the asymmetric sliding-block type, which permits a continuous variation in test section Mach number from about 2.30 to 4.70.

Model

Drawings and dimensions of the model are presented as figure 2 and table I, and photographs of the model are presented as figure 3. The wing of the configuration is a modified delta with clipped tips. The maximum thickness of the hexagonal section wing is $2\frac{1}{2}$ percent between the 50- and 70-percent chord lines. The leading edge of the wing has 62° sweepback. The ducting simulates four of the engines located in a package below the wing and the two engines located in the rearward portion of the fuselage above the wing. The inlets on the package are sized to serve all six contemplated engines. The underside of the fuselage, from forward of the inlets to about the midchord of the wing, was "scooped out" to provide

a boundary-layer bleed for the inlets. (See fig. 2.) The engine package was removable and with the package removed, tests could be made with the diverter (boundary-layer bleed) open, as designed, or faired smooth into the original fuselage contours. The fuselage has circular sides with a flat upper and lower surface.

Configuration Design Considerations

The proposed configuration, as previously mentioned, was designed to carry approximately 200 passengers. A schematic drawing of one possible arrangement is shown in figure 4. The passengers can be seated seven abreast with 18 inches allowed for each seat and with an 18-inch aisle. Three feet of longitudinal space per seat row is considered ample, thus 100 feet of length would be more than sufficient, spacewise, to accommodate the proposed passenger complement. In addition, allowances were made for necessary cloakrooms, galleys, restrooms, electronic equipment, and pilot compartment. Four inches of space were made available for insulating material around the cabin due to the anticipated heat levels in the proposed speed regime of this configuration. The cabin would be constructed as a lateral double bubble for rigidity purposes and has ample space for storage, operating equipment, and many other items. It may be noted that part of the fuel storage is in the forward portion of the fuselage. This condition means that fuel lines must be extended rearward under the cabin; however, this is believed to be a necessity for this type of configuration on the basis of balancing the weight properly to afford a center-of-gravity location far enough forward for stability purposes.

Test Conditions and Procedure

The test conditions were as follows:

Mach number	2.30	2.95	4.00	4.50
Stagnation temperature, $^{\circ}F$ . .	150	150	175	175
Stagnation dewpoint, $^{\circ}F$ . . .	<-30	<-30	<-30	<-30
Stagnation pressure, psia . .	11.4	14.6	26.9	33.9
Reynolds number based on mean aerodynamic chord of the wing	3.0×10^6	3.0×10^6	3.0×10^6	3.0×10^6

All configurations were tested through an angle-of-attack range of approximately -4° to 12° at angles of sideslip of approximately 0° and 4°. Canard angle was varied from about 0° to 3° and nose angles used were 0° and 2.5° (both measured with respect to the wing chord line).

The model, for all tests, incorporated fixed transition at the 5-percent chord of the wing, canard, and vertical surfaces. Transition was also fixed 1 inch back of and around the model nose. Transition was fixed by means of No. 60 carborundum (approximately 0.012-inch diameter) grains set in a plastic adhesive about 1/16 inch wide except on the nose and lower surface of the canard where it was composed of 0.031-inch grains of sand spaced approximately 0.1 inch apart.

Measurements

Aerodynamic forces and moments were determined by means of a six-component electrical strain-gage balance housed within the fuselage. The balance, in turn, was rigidly fastened to a sting support system, and provision was made to detect any fouling between the model and sting support system.

Balance chamber pressure was measured by means of a single static orifice located in the vicinity of the strain-gage balance. Duct exit pressure was determined on one side of the model by means of a total-pressure probe placed about 1/4 inch inside the duct exit. A check to determine the existence of sonic flow at the duct exit was made by means of a static-pressure orifice located in the proximity of the local total-pressure probe. (The duct exit was sized to obtain sonic flow and thereby facilitate computations of internal drag.)

Corrections

Corrections to the indicated model angle of attack have been made for both tunnel air-flow misalinement and deflection of model and sting support due to aerodynamic load.

The drag data presented herein have been adjusted to correspond to zero balance chamber drag coefficient. In addition, the internal drag has been subtracted from the adjusted drag values and the drag coefficients presented in this paper represent the net external drag of the model. The magnitude of these drag adjustments may be found in figure 5.

Accuracy

Based upon balance calibration and repeatability of data, it is estimated that the various measured quantities are accurate within the following limits:

C_A	±0.0005
C'_D	±0.0005
$C'_{D,c}$	±0.0002
$C'_{D,i}$	±0.0002
C_L	±0.002
C_l	±0.0002
C_m	±0.001
C_n	±0.0005
C_Y	±0.002
M:	
Between 2.30 and 4.00	±0.015
Above 4.00	±0.05
α, deg	±0.1
β, deg	±0.1

PRESENTATION OF RESULTS

	Figure
Effect of canard on aerodynamic characteristics in pitch	6
Effect of engine package and diverter on aerodynamic characteristics in pitch ($\delta_n = 0^\circ$, $\delta_c = -0.5^\circ$)	7
Summary of longitudinal characteristics	8
Effect of nose deflection on variation of C_A with angle of attack (M = 2.95)	9
$(L/D)_{max}$ extrapolation from model to full scale	10
Variation of lateral characteristics with angle of attack:	
For $\delta_n = 0^\circ$	11
For $\delta_n = 2.5^\circ$	12
Engine package off; diverter open; $\delta_n = 0^\circ$; $\delta_c = -0.5^\circ$	13
Summary of lateral characteristics	14

DISCUSSION

Longitudinal Characteristics

Lift.- The data presented in figure 6 show the familiar reduction in lift-curve slope with increasing Mach number for the configuration with the nose either at 0° or deflected 2.5°. Deflecting the canard approximately 3° has no significant effect on C_{L_α} or C_{L_o} in the

test Mach number range for the configuration with either nose deflection. Deflecting the nose 2.5° leads to a slight increase in C_{L_o}; however, the lift-curve slope remains unchanged. Tests of the configuration with the canard removed were only performed over a very small angle-of-attack range due to the model fouling against the sting support under high pitching-moment loads. The limited data obtained, however, indicate little or no change in C_{L_α} or C_{L_o} due to removing the canard. It would be expected that the canard would carry some of the lift load, but because of its small size (dictated by the moment arm afforded by the long forebody component), the additive lift of the canard is masked by the test accuracy.

There are no significant changes in any of the lift parameters due to removing the engine package or fairing the diverter smooth with the body contours. (See fig. 7.) This result indicates that there is little or no benefit due to interference effects derived from any high-pressure flow field that may be produced by the engine package on the underside of the wing.

Pitch.- The basic configuration is approximately neutrally stable about the center of gravity used for these tests throughout the test Mach number range. At $M = 2.95$, the data indicate a static margin of about 2 percent. The center of gravity of the configuration could be moved forward to provide suitable stability by proper arrangement of fuel storage. The data of figure 8 indicate that the canard reduces the static margin of the configuration by about 16 percent at $M = 2.95$. The effectiveness of the canard in producing the positive C_{m_o}, necessary to trim at $(L/D)_{max}$ values, is not quite as good as that of nose deflection, particularly at the higher test Mach numbers. For example, at $M = 2.95$, C_{m_o} per degree δ_c is approximately equal to 0.0022 and C_{m_o} per degree δ_n is approximately equal to 0.004. At $M = 4.5$, C_{m_o} per degree δ_c is approximately equal to 0.0012 and C_{m_o} per degree δ_n is approximately equal to 0.003. It should be pointed out that some of the superiority of the nose over the canard in producing C_{m_o} is due to the larger planform area of the nose.

The data shown in figure 7 indicate that the engine package and the diverter only contribute secondary effects on any of the pitch parameters of the configuration.

Drag and performance.- The configuration with the nose and the canard at 0° has a minimum drag coefficient of 0.0114 at $M = 2.95$ (near design cruise speed) and a maximum lift-drag ratio of about 5.6 or 5.7. (See fig. 8.) An increase in Mach number to 4.5 has no significant effect on the value of $(L/D)_{max}$ for the basic configuration. Deflecting the

canard approximately 3° leads to a decrease in $(L/D)_{max}$ of about 0.1 throughout the test Mach number range, although there is little change in minimum drag coefficient. Deflecting the nose of the configuration 2.5° leads to a decrease in $(L/D)_{max}$ of about 0.3. This is in contrast to data from other sources (for example, ref. 4) that indicate little or no change in $(L/D)_{max}$ due to nose deflections of this magnitude. The results presented in figure 9 show that this adverse effect of the nose is reflected in the axial-force coefficients of the configuration. With the nose at 0°, the axial-force coefficients "bucket" near $\alpha = 0^{\circ}$; however, with $\delta_n = 2.5^{\circ}$, the axial-force coefficients continually increase from the most negative test angle of attack. There is considerable difference in C_A near $(L/D)_{max}$ for the two nose configurations. Unpublished data indicate that this adverse effect of nose deflection on axial-force coefficient may be associated with the blunt plan form of the nose and would be minimized or possibly eliminated by changing the plan form to a pointed or ogival shape. More test results are needed, however, to validate this phenomenon. Although the drag penalty is less for deflecting the nose than for deflecting the canard, unpublished data have indicated that C_{m_o} can be more efficiently obtained by using a combination of smaller canard deflections with smaller nose deflections than were used for the present investigation.

Figure 8 shows that the penalty in $(L/D)_{max}$ for the diverter is between 0.2 and 0.3 throughout the test Mach number range. The penalty in $(L/D)_{max}$ for the engine package is about 0.3 at Mach numbers of 2.3 and 2.95; however, there is little or no difference in the values of $(L/D)_{max}$ between the configurations with or without the engine package at Mach numbers of 4.0 and 4.5. Refinements to the engine package and diverter will possibly lead to wind-tunnel maximum lift-drag ratios approaching 6 at $M = 3.0$, and it is believed that the configuration can be trimmed with suitable static margin to produce a maximum lift-drag ratio near this value.

Figure 10 shows the variation of $(L/D)_{max}$ with Mach number for the untrimmed test configuration ($R = 3 \times 10^6$) and for the estimated full-scale configuration flying at altitudes compatible with the lift coefficient for $(L/D)_{max}$ of the configuration (if $W/S_w \approx 70$ lb/sq ft). Near a Mach number of 3, the $(L/D)_{max}$ for the full-scale configuration would be about 6.8. This explanation is based on the assumption that full-scale surface conditions will approach those of the model and that drag extrapolations based on existing turbulent Reynolds number theory are valid. With the aforementioned refinements to the engine package and diverter a full-scale $(L/D)_{max}$ of 7 or greater may be obtained.

[redacted]

A value of about 7 for (L/D) has previously been mentioned in the Introduction as that necessary for an economically feasible Mach number 3 transport configuration.

In order to determine, to the first order, whether any undue drag due to lift is being encountered by the configurations, the drag due to lift of the test configurations has been compared with that for a two-dimensional, triangular wing (supersonic leading edge). This comparison (fig. 8) generally shows close agreement between the model results and theory at all test Mach numbers. A comparison of the drag due to lift of the test configurations with those of a theoretical flat plate is also shown in figure 8. The test configurations have a somewhat lower drag due to lift at $M = 2.30$, and this trend reduces with Mach number and disappears at $M = 4.50$.

L
6
6
6

Lateral and Directional Stability

With the nose and canard of the configuration at approximately 0° with respect to the wing chord line, the configuration is directionally stable throughout the test angle-of-attack range for $M = 2.3$. (See figs. 11 and 13.) At a Mach number of 2.95, the configuration is directionally unstable at angles of attack between approximately $\pm 3^\circ$. At the two higher test Mach numbers, the configuration is directionally unstable at angles of attack between approximately $\pm 4^\circ$. The degree of directional instability in all of these instances is relatively low and does not exceed a value of $\Delta C_n/\Delta\beta = 0.00025$. Canard or nose deflection of 2.5° has little or no effect on the directional stability characteristics of the configuration. Removing the canard, also, has little effect on the directional stability characteristics of the configuration.

For the configuration with the nose and canard at 0°, a negative dihedral effect is produced at all negative test angles of attack and at angles of attack up to approximately 2° for $M = 2.3$. Increasing the Mach number increases the angle of attack at which a positive dihedral effect begins. Deflecting the canard or nose 2.5° leads to a reduction in angle of attack at which a positive dihedral effect begins at all test Mach numbers; for example, at $M = 2.3$ with both the nose and canard deflected 2.5°, positive dihedral is effected at all positive angles of attack.

Removing the engine package leads to a slight increase in directional stability for the configuration and considerably increases the negative dihedral effect. (See fig. 13.)

A forward shift of the center of gravity by $0.05\bar{c}$ coupled with a pointed or ogived nose plan form will produce a static margin of more than 7 percent at $M = 3.0$. This amount of center-of-gravity shift, in

turn, will also lead to a directionally stable configuration and more nearly place the center of gravity of the configuration in the center of the passenger compartment (a desirable airliner feature).

CONCLUDING REMARKS

Tests of a model of a canard-type transport configuration have indicated maximum lift-drag ratios of about 5.7 near a Mach number of 3 at a Reynolds number of 3×10^6. An experimental trimmed lift-drag ratio approaching 6 is deemed to be possible through further refinements to this configuration. On a basis of aerodynamic efficiency, this proposed Mach number 3 transport would be economically feasible since the lift-drag ratios will approach and possibly exceed 7 for flight conditions if the full-scale surface conditions are compatible with model surface conditions.

Langley Research Center,
National Aeronautics and Space Administration,
Langley Field, Va., October 15, 1959.

REFERENCES

1. Anon.: Supersonic Transports (Proceedings). S.M.F. Fund No. FF-20, Inst. Aero. Sci., Jan. 1959.

2. Jones, J. L., and Dennis, D. H.: Mach 3-5 Airliners Look Economically Feasible. Space Aero., vol. 31, no. 4, Apr. 1959, pp. 41-43.

3. Baals, Donald D., Toll, Thomas A., and Morris, Owen G.: Airplane Configurations for Cruise at a Mach Number of 3. NACA RM L58E14a, 1958.

4. Spearman, M. Leroy: Some Factors Affecting the Static Longitudinal and Directional Stability Characteristics of Supersonic Aircraft Configurations. NACA RM L57E24a, 1957.

TABLE I.- MODEL DESIGN DIMENSIONS

Wing:	
Area, sq ft	1.79
Span, in.	15.272
Root chord, in.	24.657
Tip chord, in.	10.298
Aspect ratio	0.905
Taper ratio	0.417
Mean aerodynamic chord, in.	18.462
Leading-edge sweep, deg	62
Airfoil section	Hexagonal section
Thickness ratio (with $(t/c)_{max}$ at 0.5c to 0.7c)	0.025
Canard:	
Area (total), sq ft	0.182
Area (exposed), sq ft	0.088
Span, in.	7.836
Root chord, in.	5.568
Tip chord, in.	1.148
Aspect ratio	4.860
Taper ratio	0.206
Mean aerodynamic chord	3.844
Leading-edge sweep, deg	45
Airfoil section	Double wedge
Thickness ratio (with $(t/c)_{max}$ at 0.6c)	0.025
Vertical wingtip fins:	
Area, each, sq ft	0.119
Center-of-gravity location, percent overall length	65.5
Center-of-gravity location, percent of mean aerodynamic chord	19.5

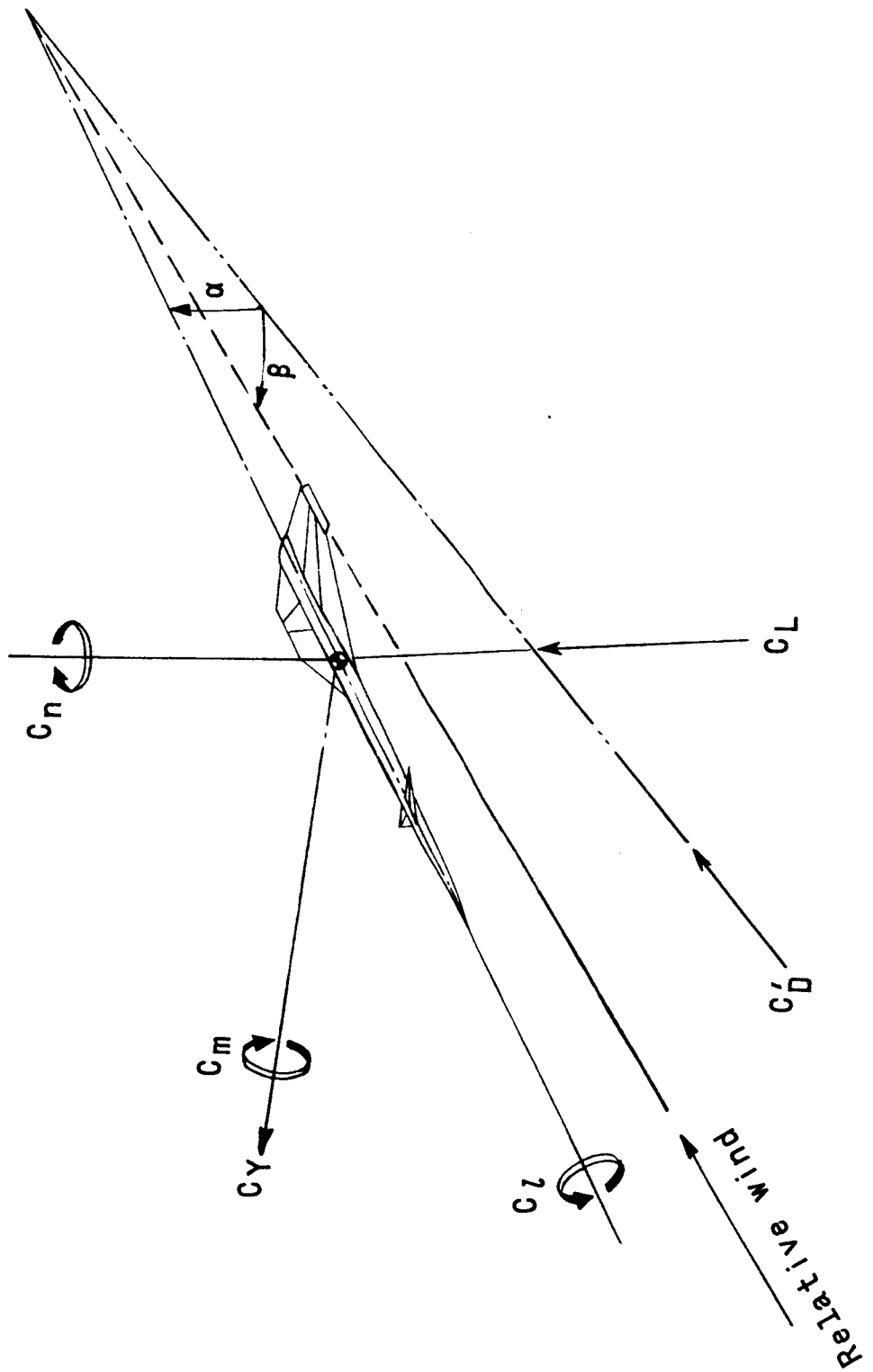

Figure 1.- Axes systems. Arrows indicate positive directions.

[redacted]

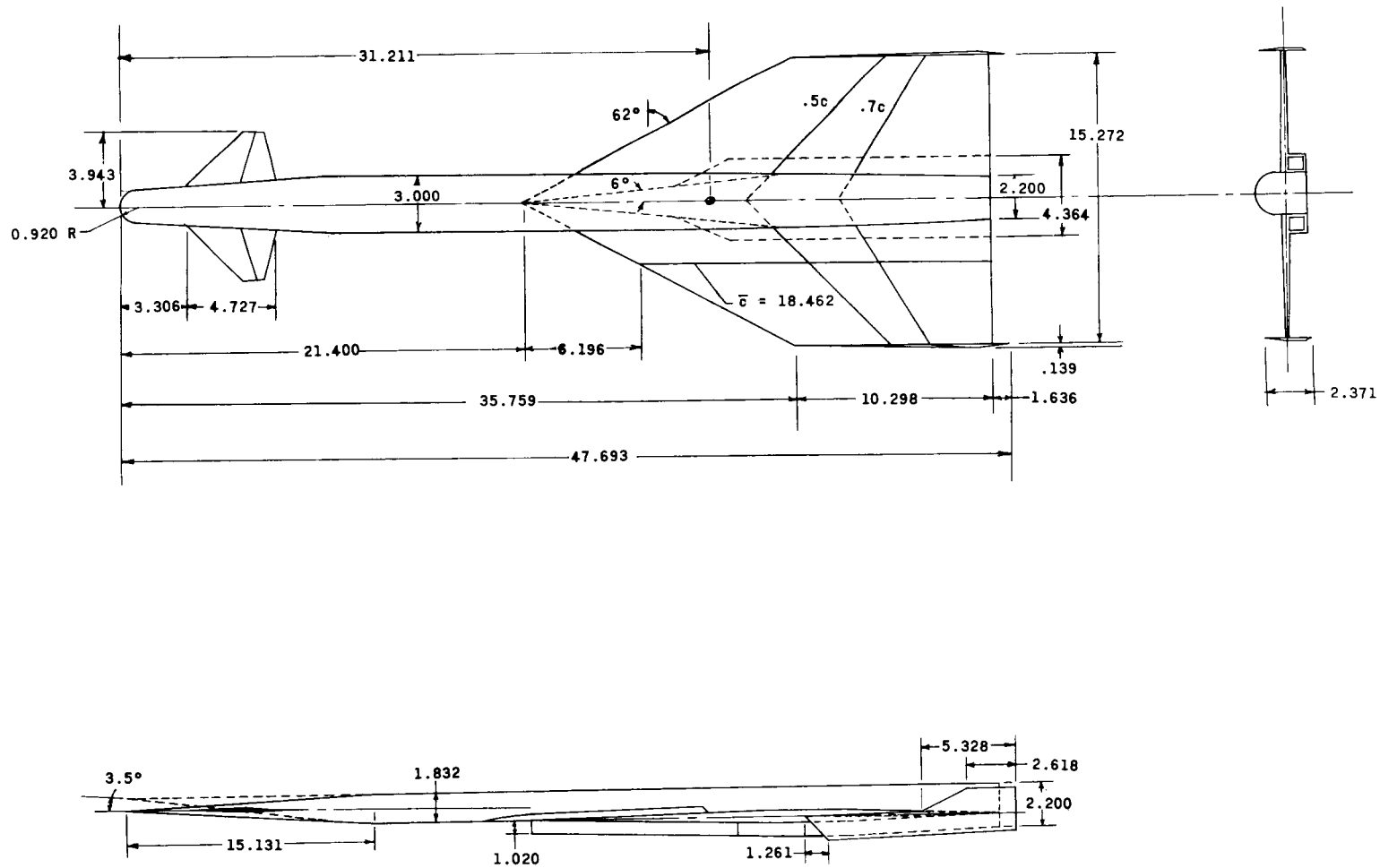

Figure 2.- Three-view drawing of test configuration. All dimensions are in inches unless otherwise noted.

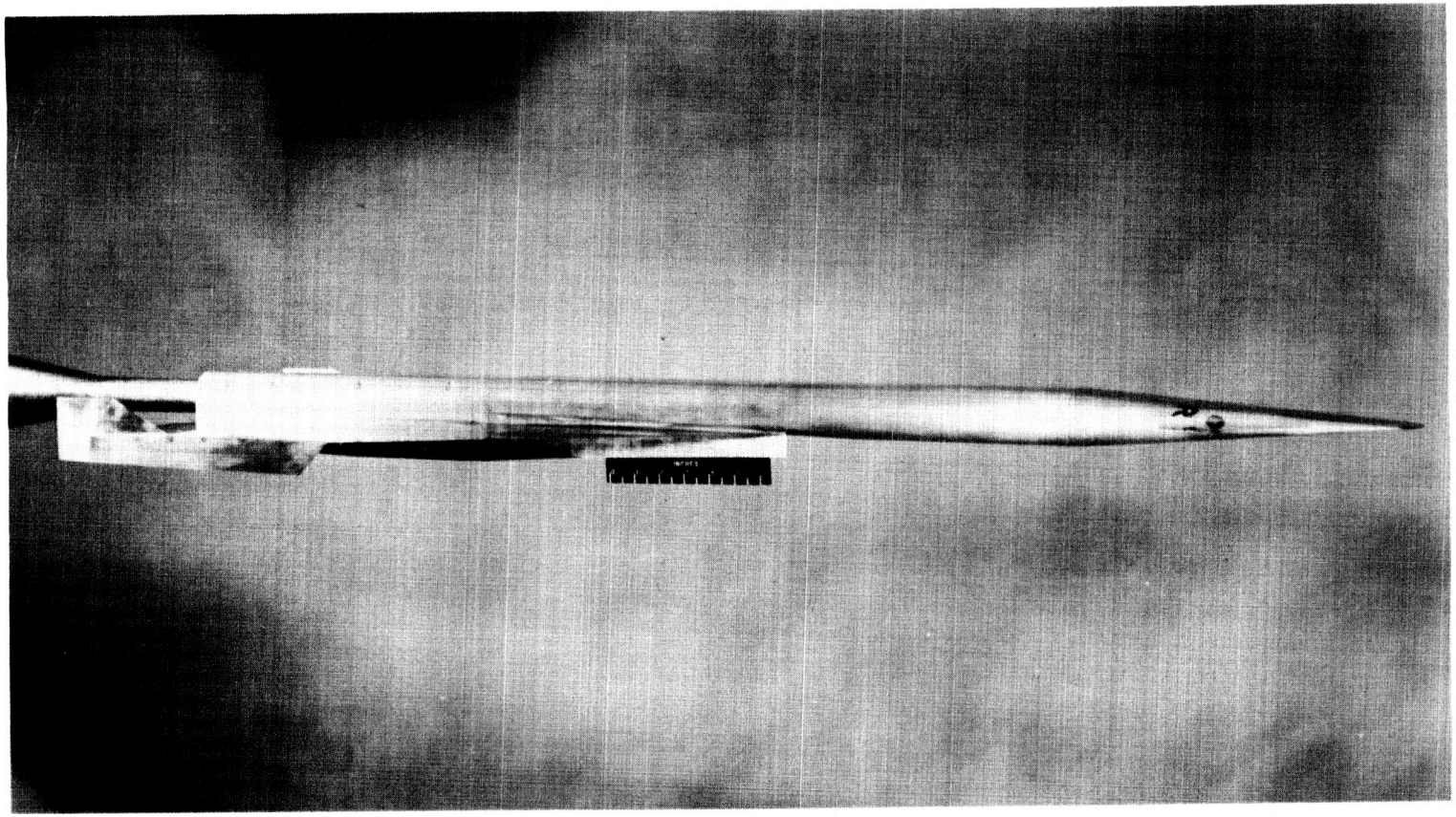

(a) Three-quarter front view. L-59-380

Figure 3.- Photographs of the test configuration.

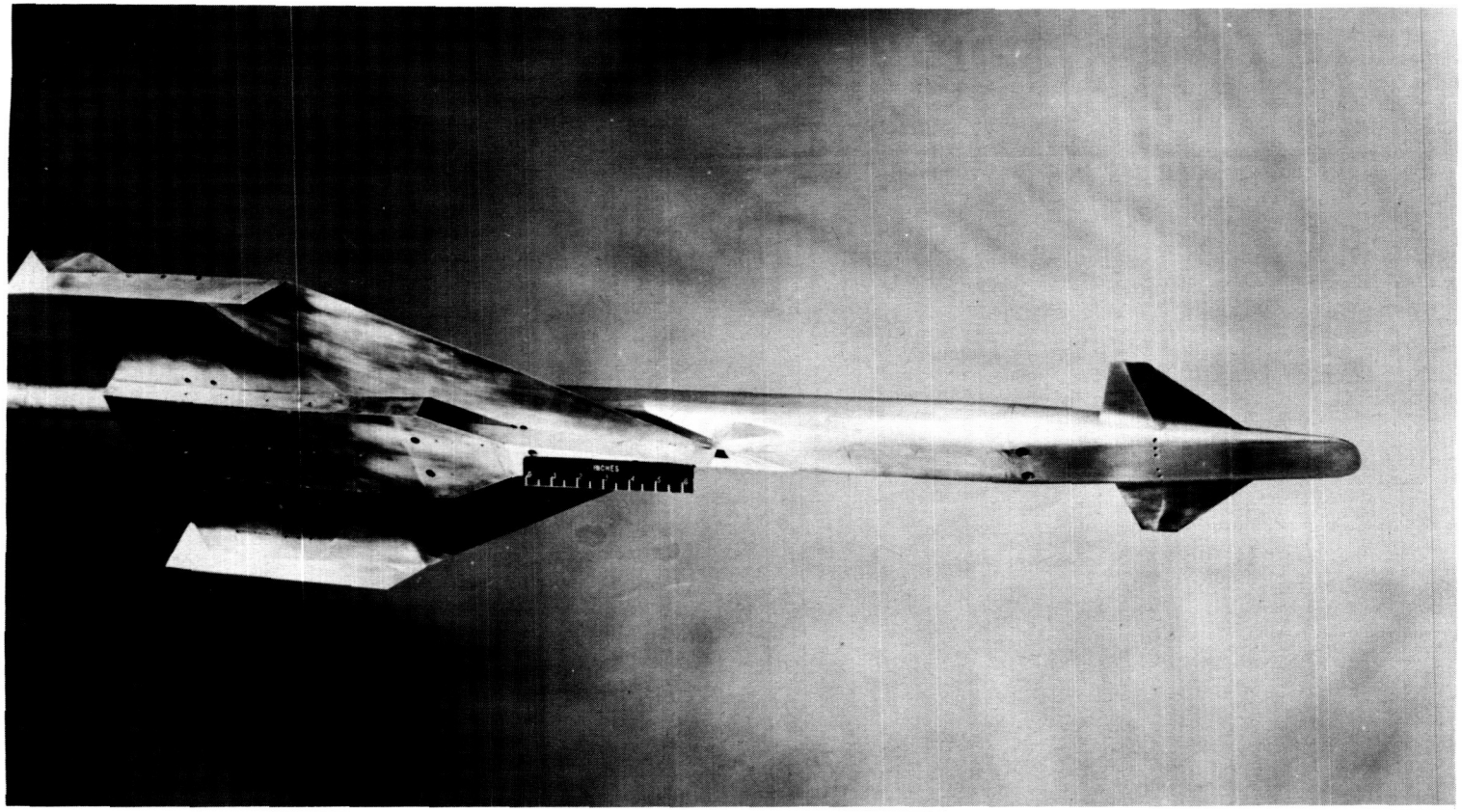

(b) Three-quarter underside view. L-59-379

Figure 3.- Continued.

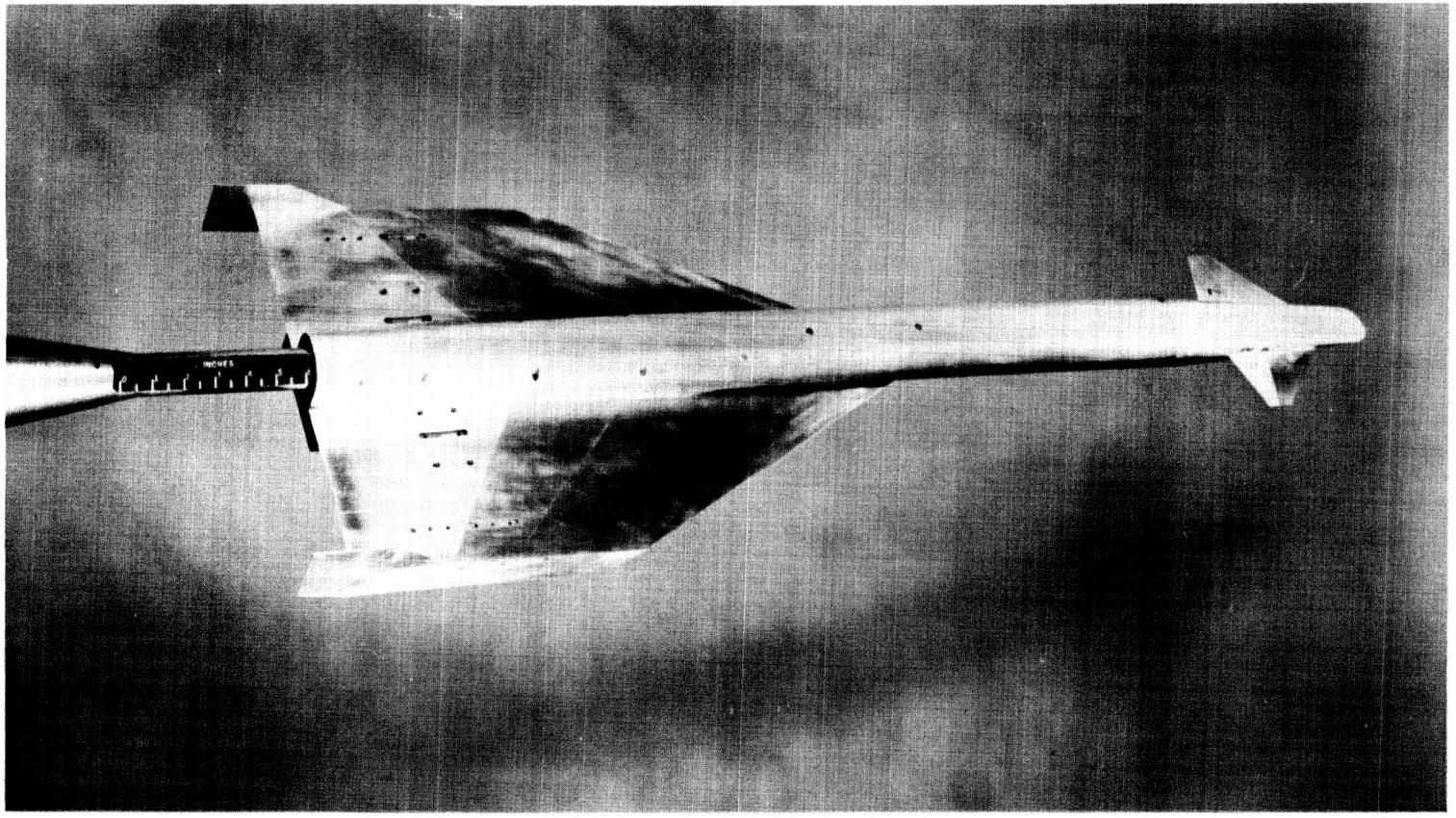

(c) Three-quarter top rear view. L-59-378

Figure 3.- Concluded.

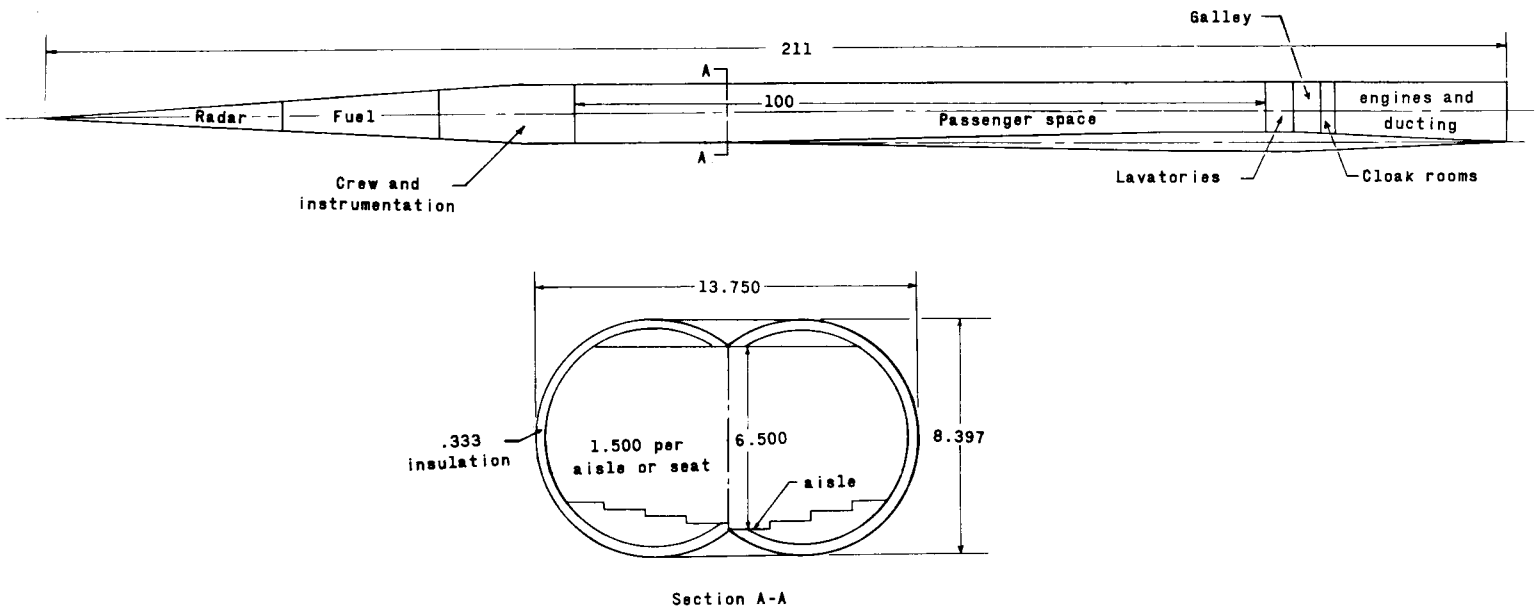

Figure 4.- A possible fuselage arrangement for crew and passengers. All dimensions are in feet unless otherwise noted.

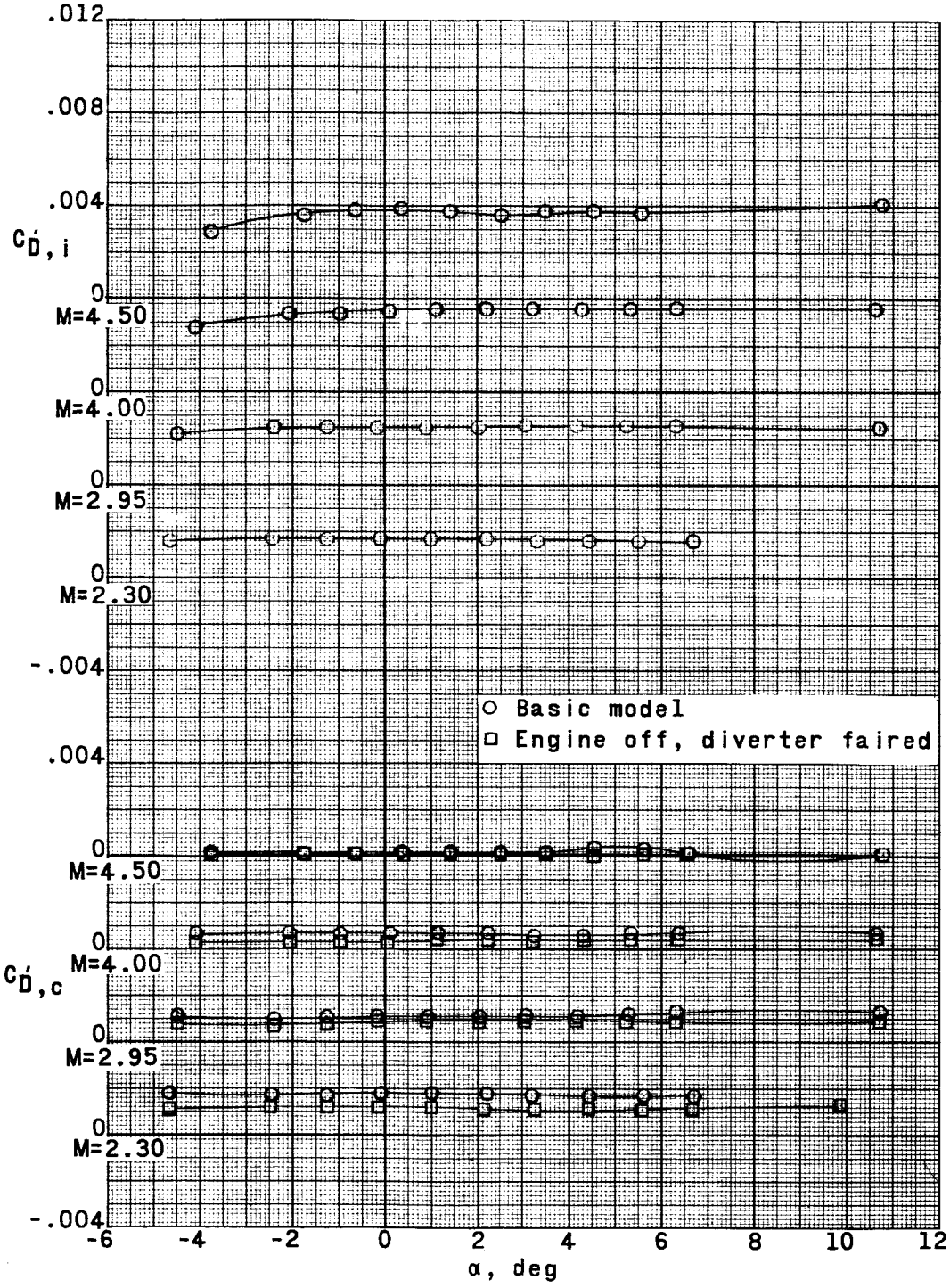

Figure 5.- Variation of $C'_{D,c}$ and $C'_{D,i}$ with α.

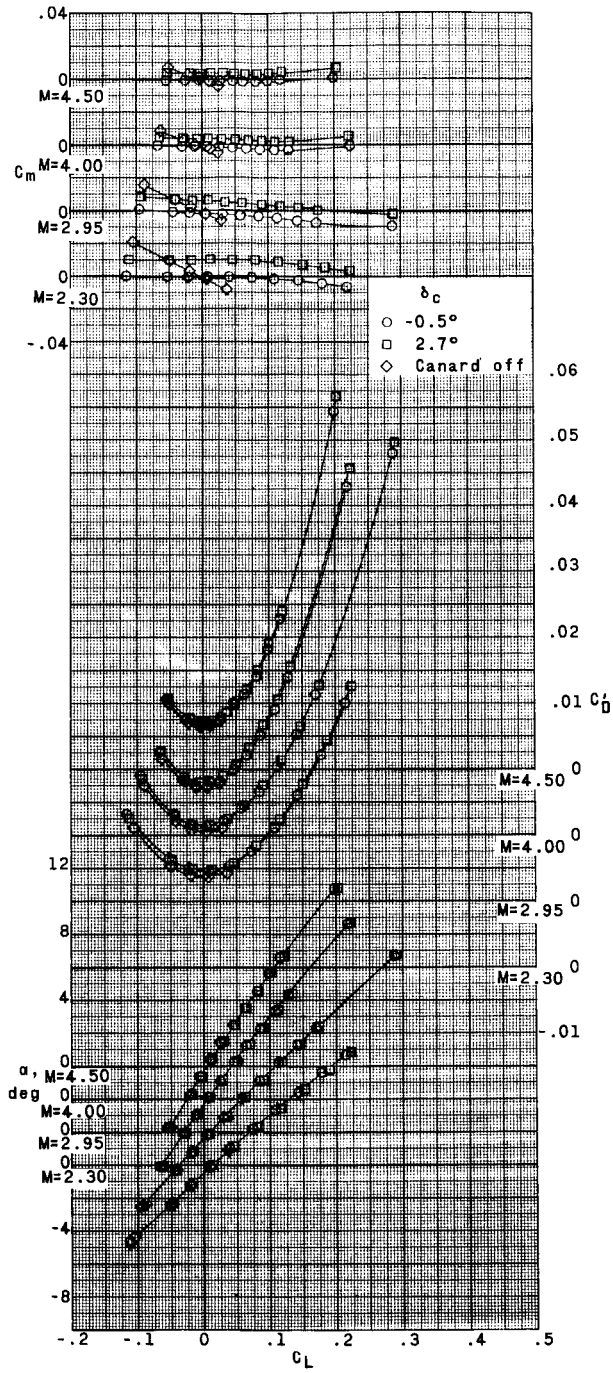

(a) $\delta_n = 0^o$.

Figure 6.- Effect of canard on aerodynamic characteristics in pitch.

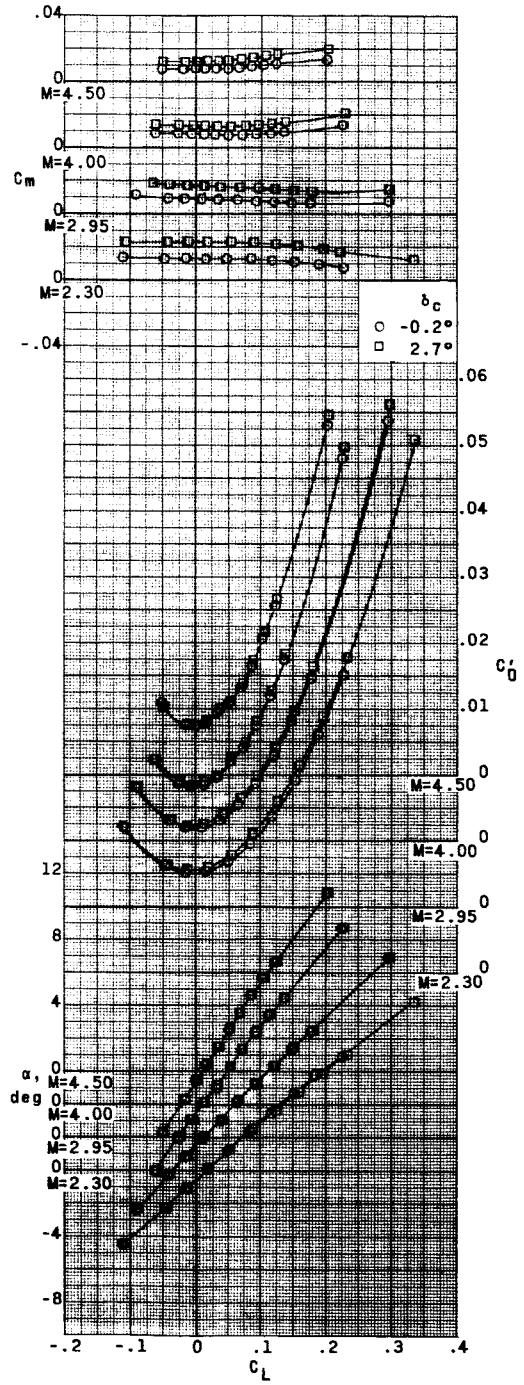

(b) $\delta_n = 2.5^o$.

Figure 6.- Concluded.

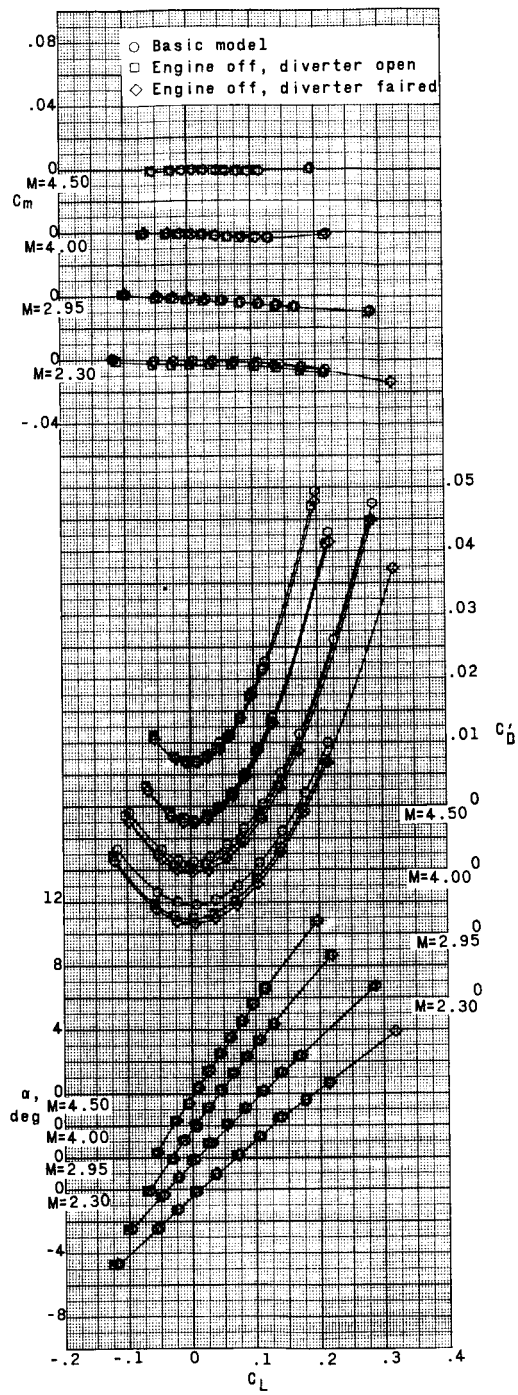

Figure 7.- Effect of engine package and diverter on aerodynamic characteristics in pitch. $\delta_n = 0^o$; $\delta_c = -0.5^o$.

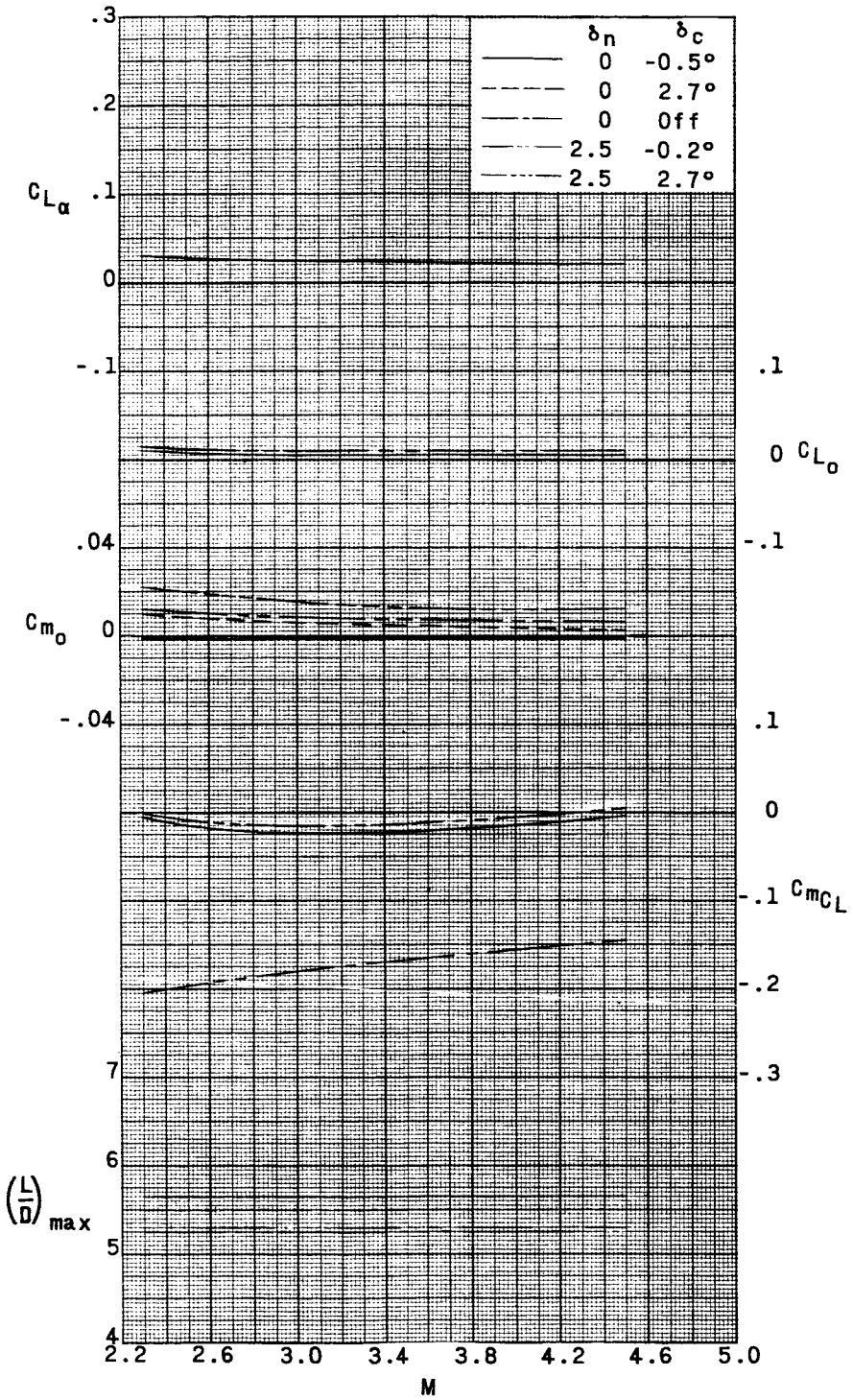

Figure 8.- Summary of longitudinal characteristics.

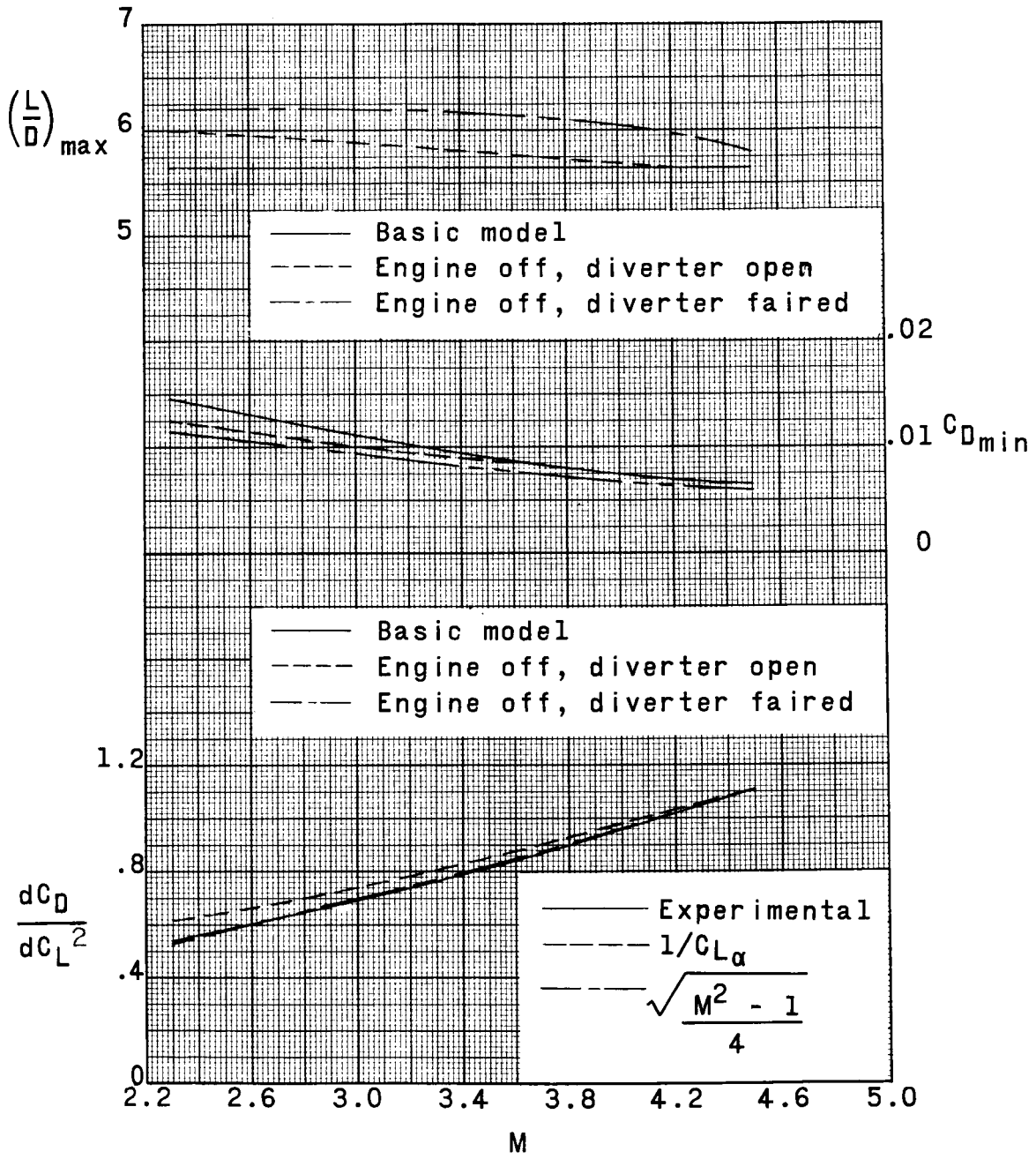

Figure 8.- Concluded.

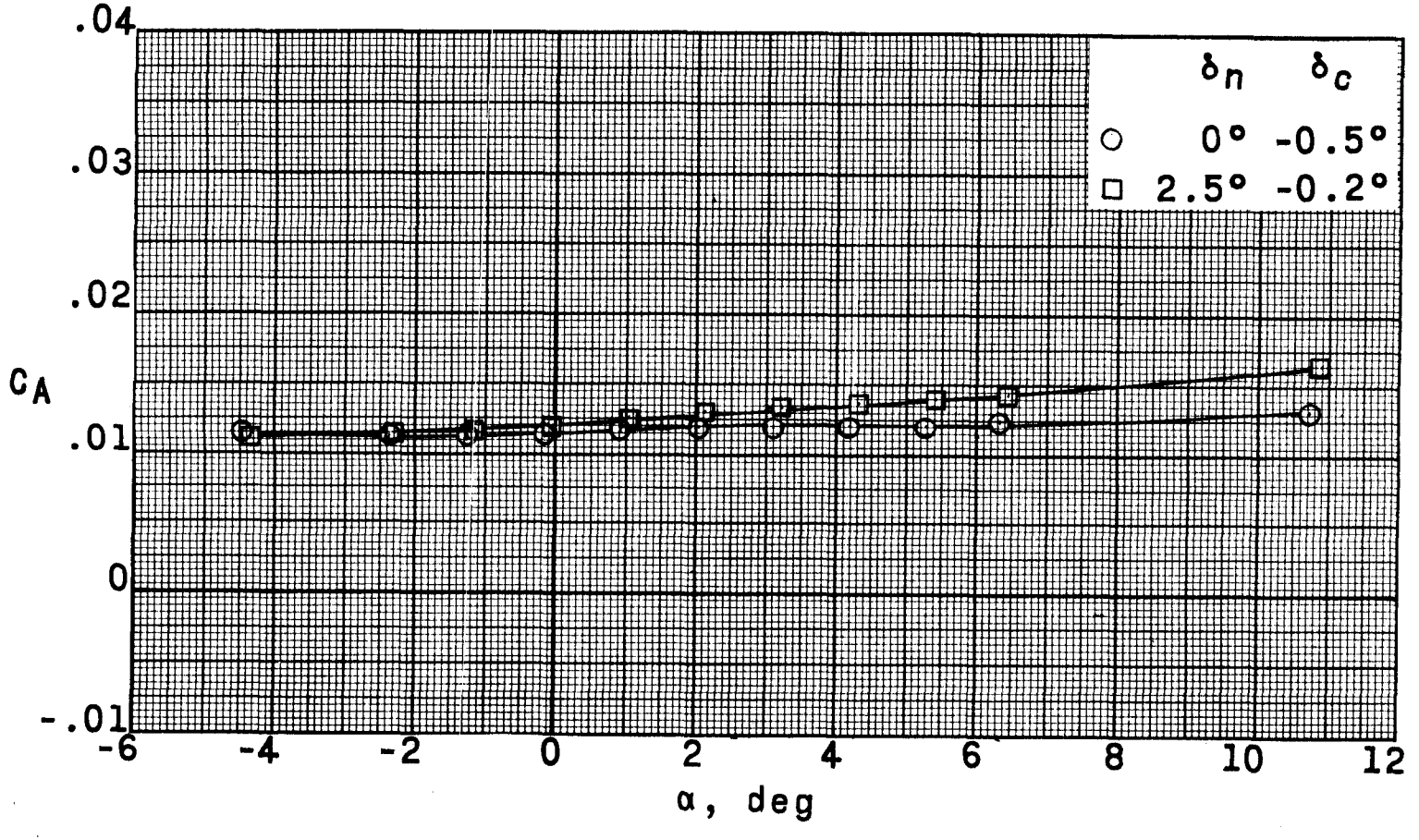

Figure 9.- Effect of nose deflection on variation of C_A with angle of attack. M = 2.95.

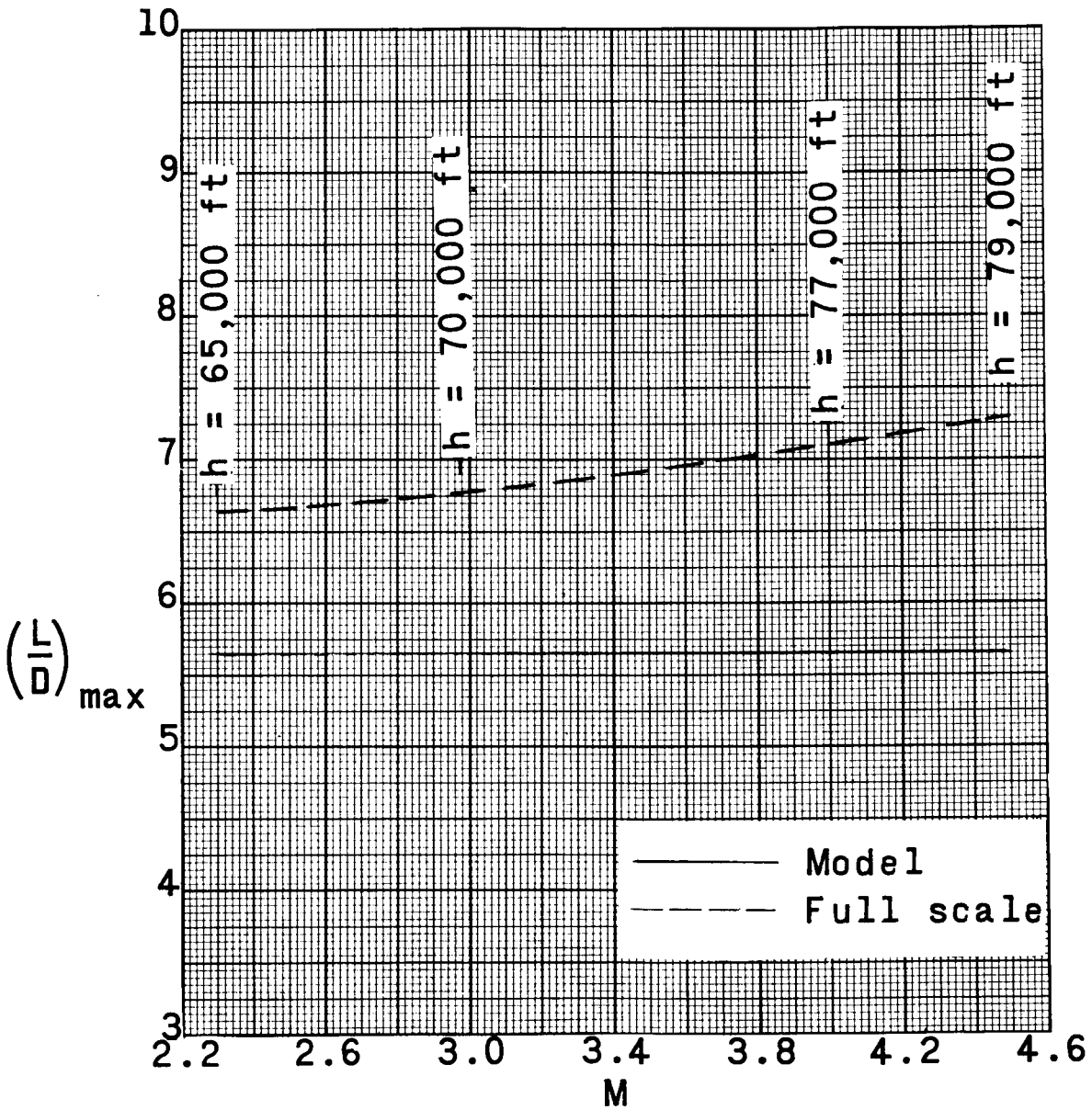

Figure 10.- $(L/D)_{max}$ extrapolation from model to full scale.

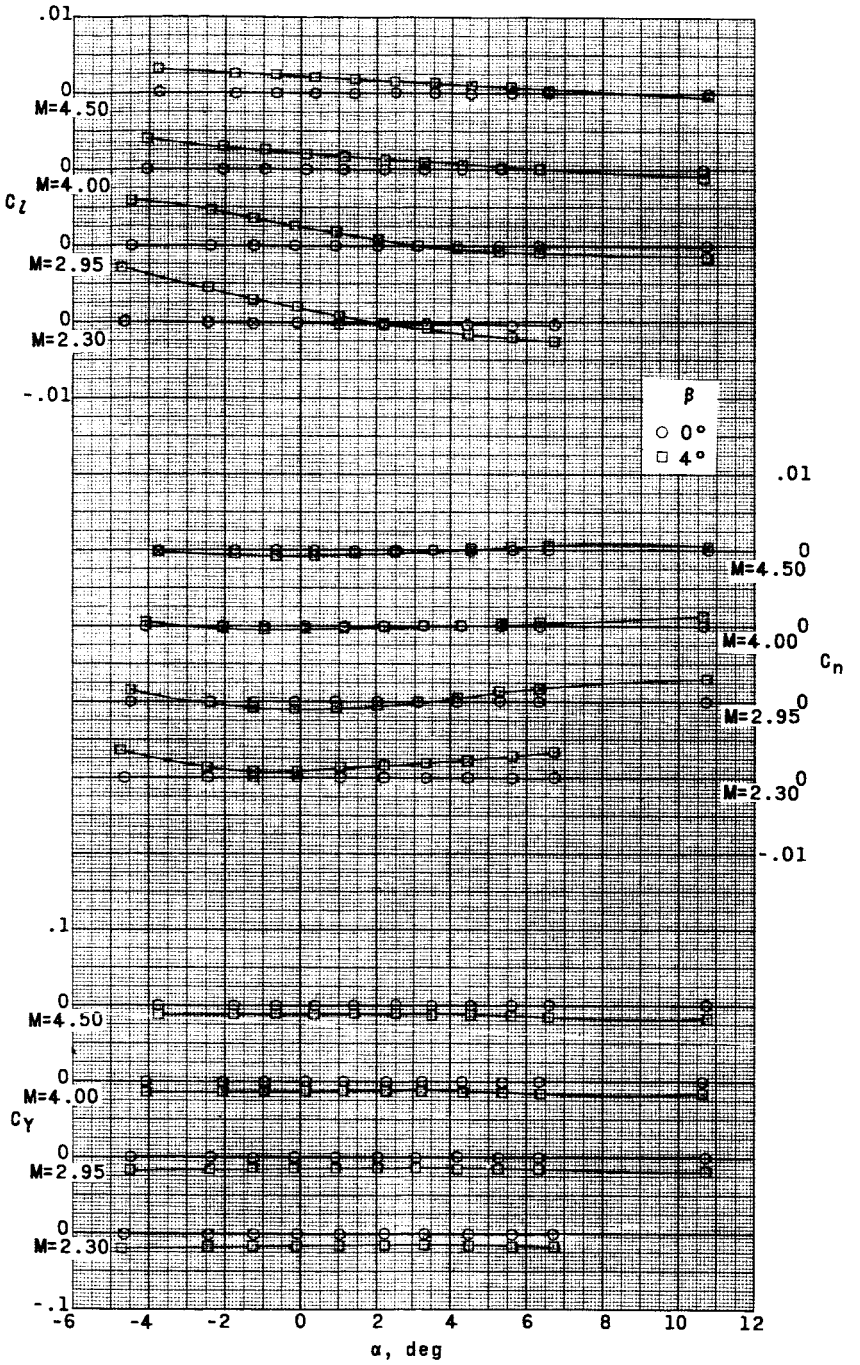

(a) $\delta_c = -0.5^\circ$.

Figure 11.- Variation of lateral characteristics with angle of attack. $\delta_n = 0^\circ$.

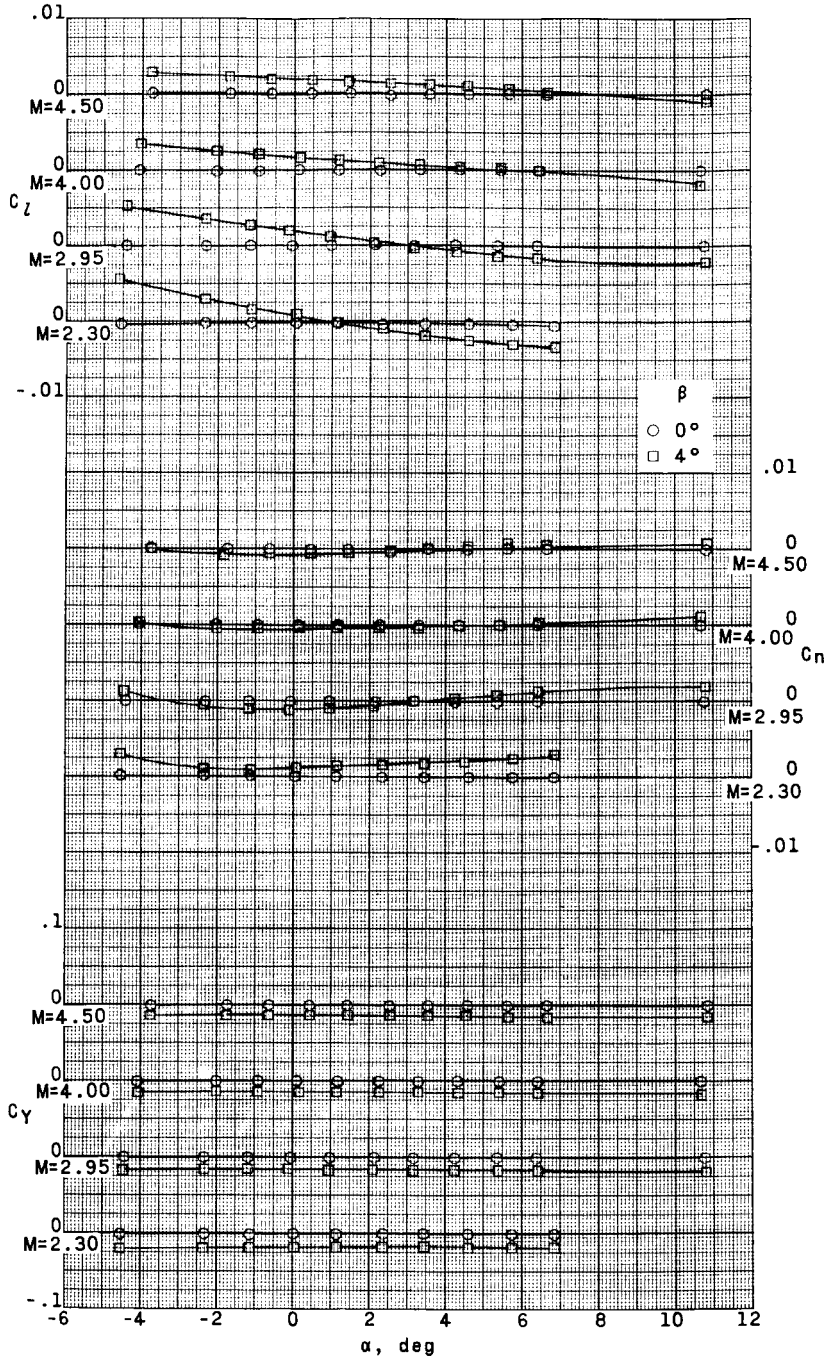

(b) $\delta_c = 2.7^o$.

Figure 11.- Continued.

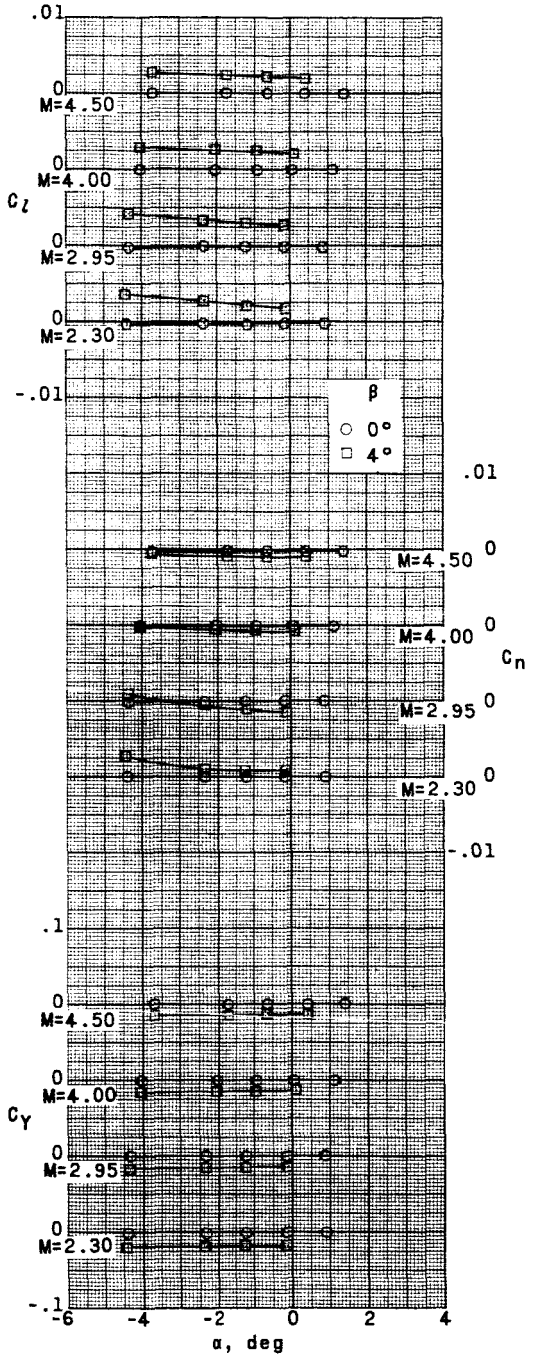

(c) Canard off.

Figure 11.- Concluded.

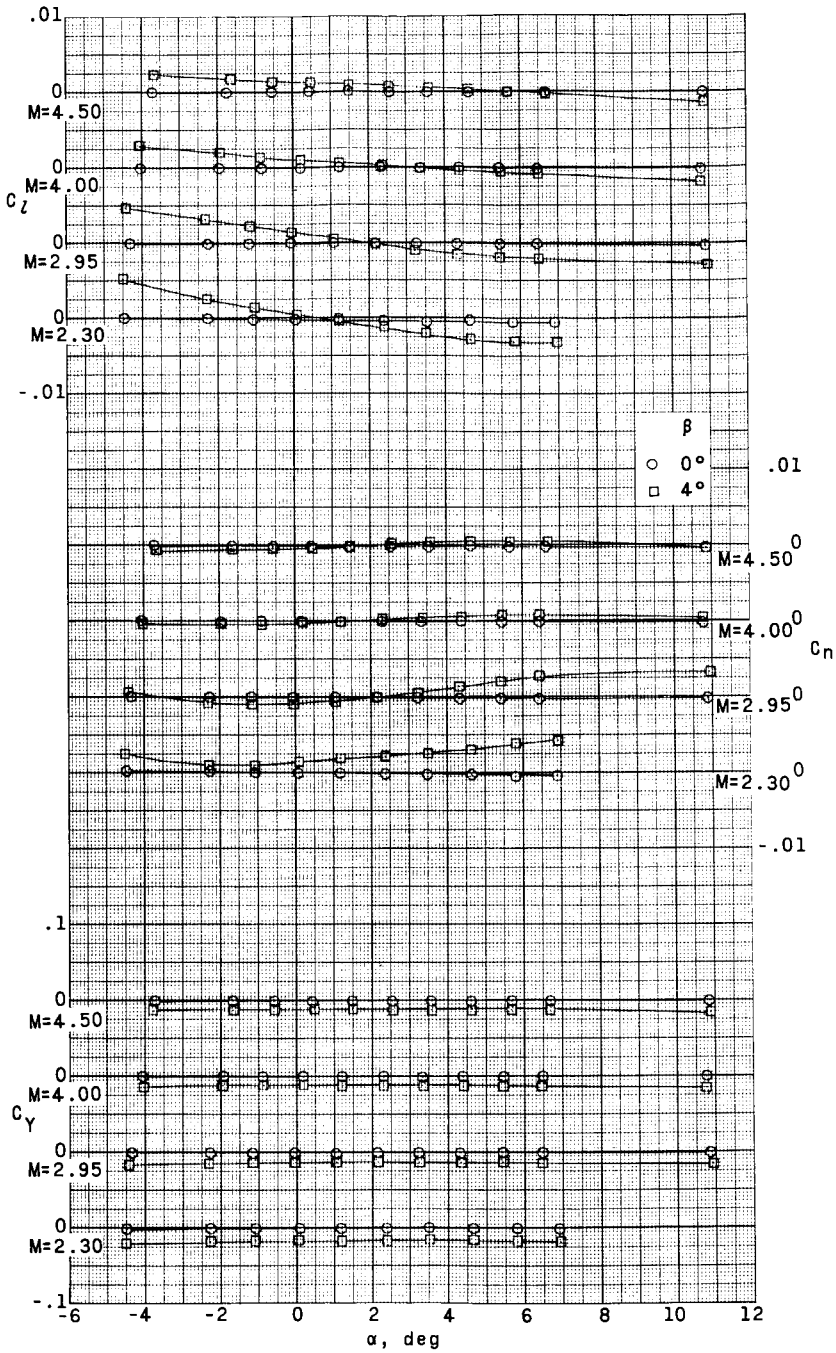

(a) $\delta_c = -0.2^\circ$.

Figure 12.- Variation of lateral characteristics with angle of attack. Complete configuration; $\delta_n = 2.5^\circ$.

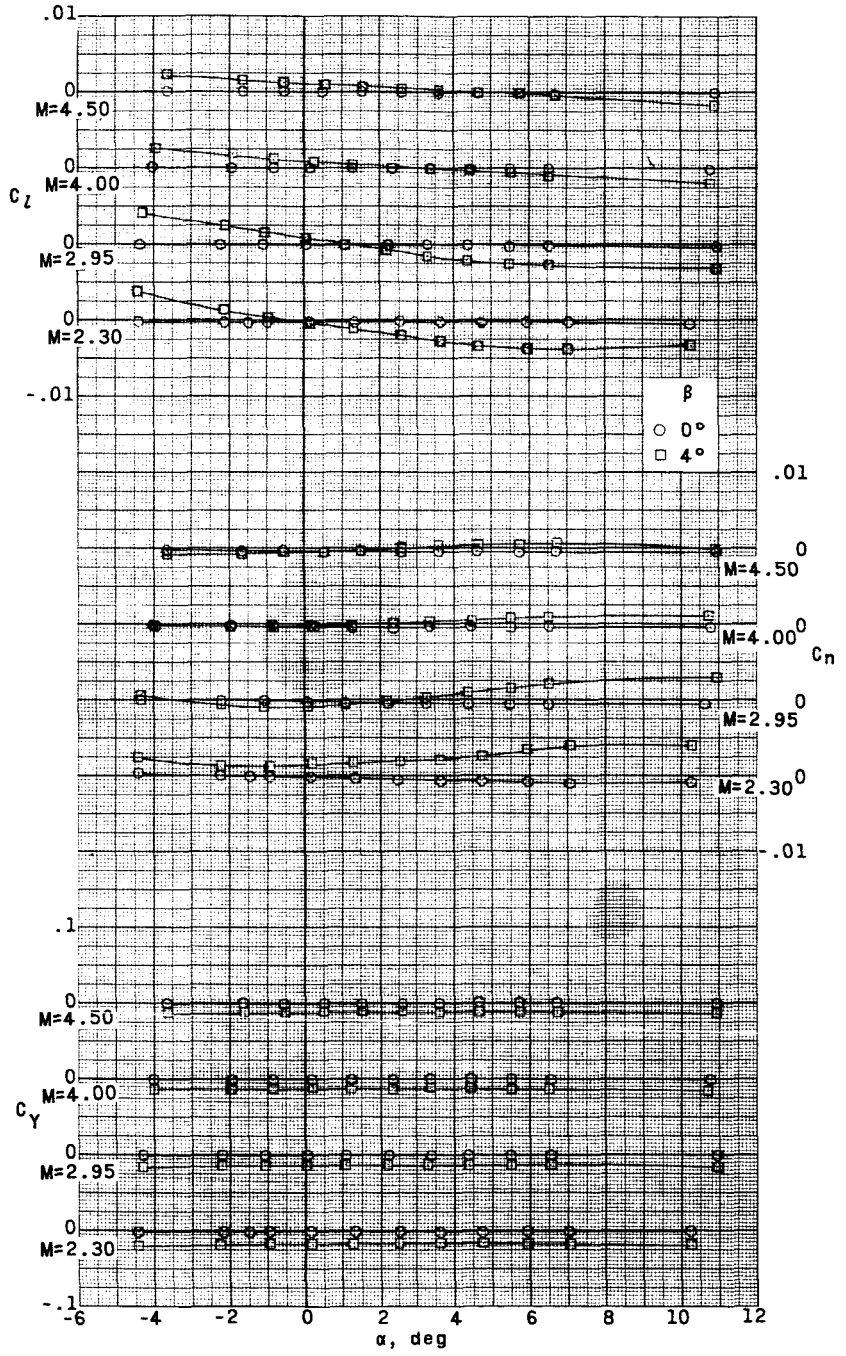

(b) $\delta_c = 2.7^\circ$.

Figure 12.- Concluded.

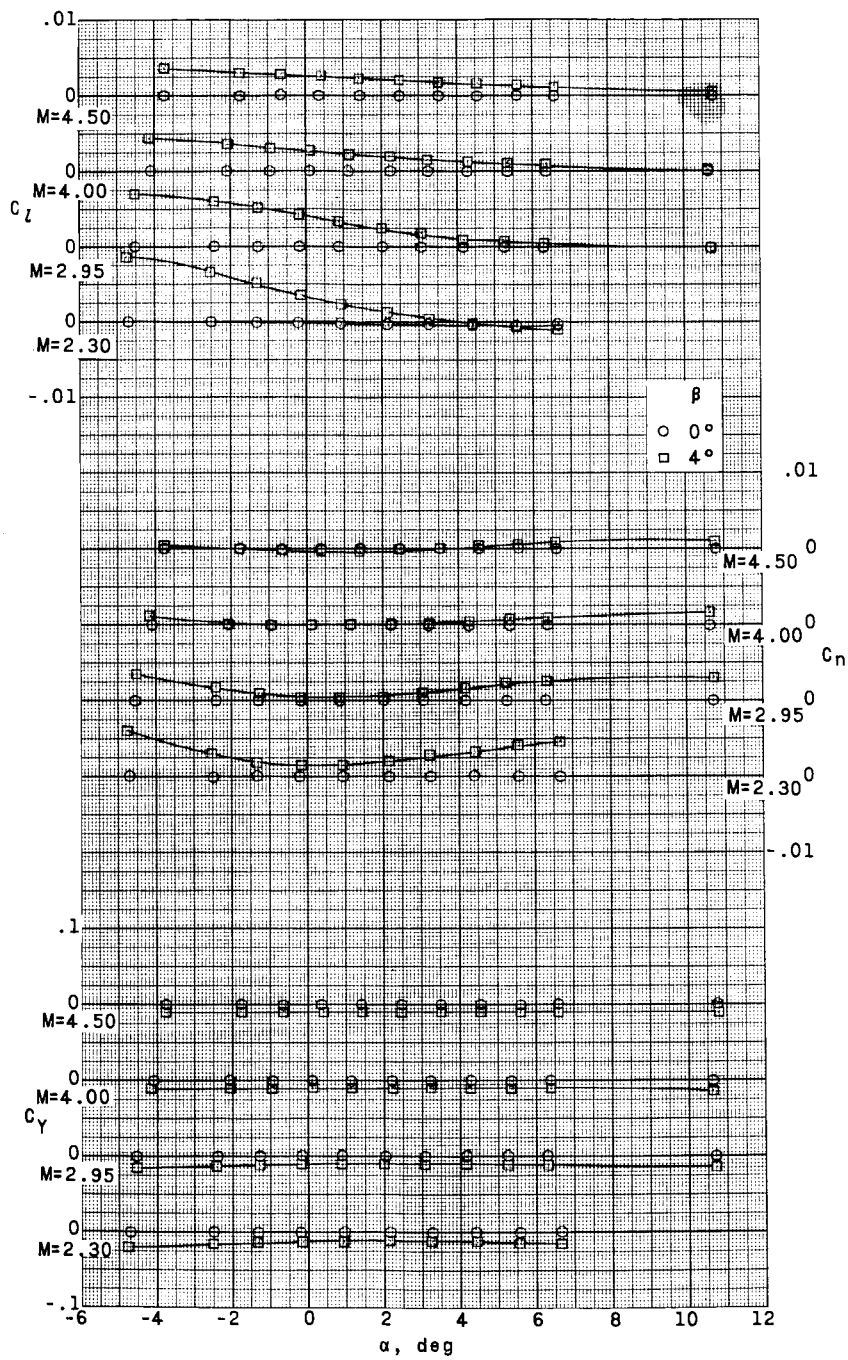

Figure 13.- Variation of lateral characteristics with angles of attack. Engine off, diverter open; $\delta_n = 0^o$; $\delta_c = -0.5^o$.

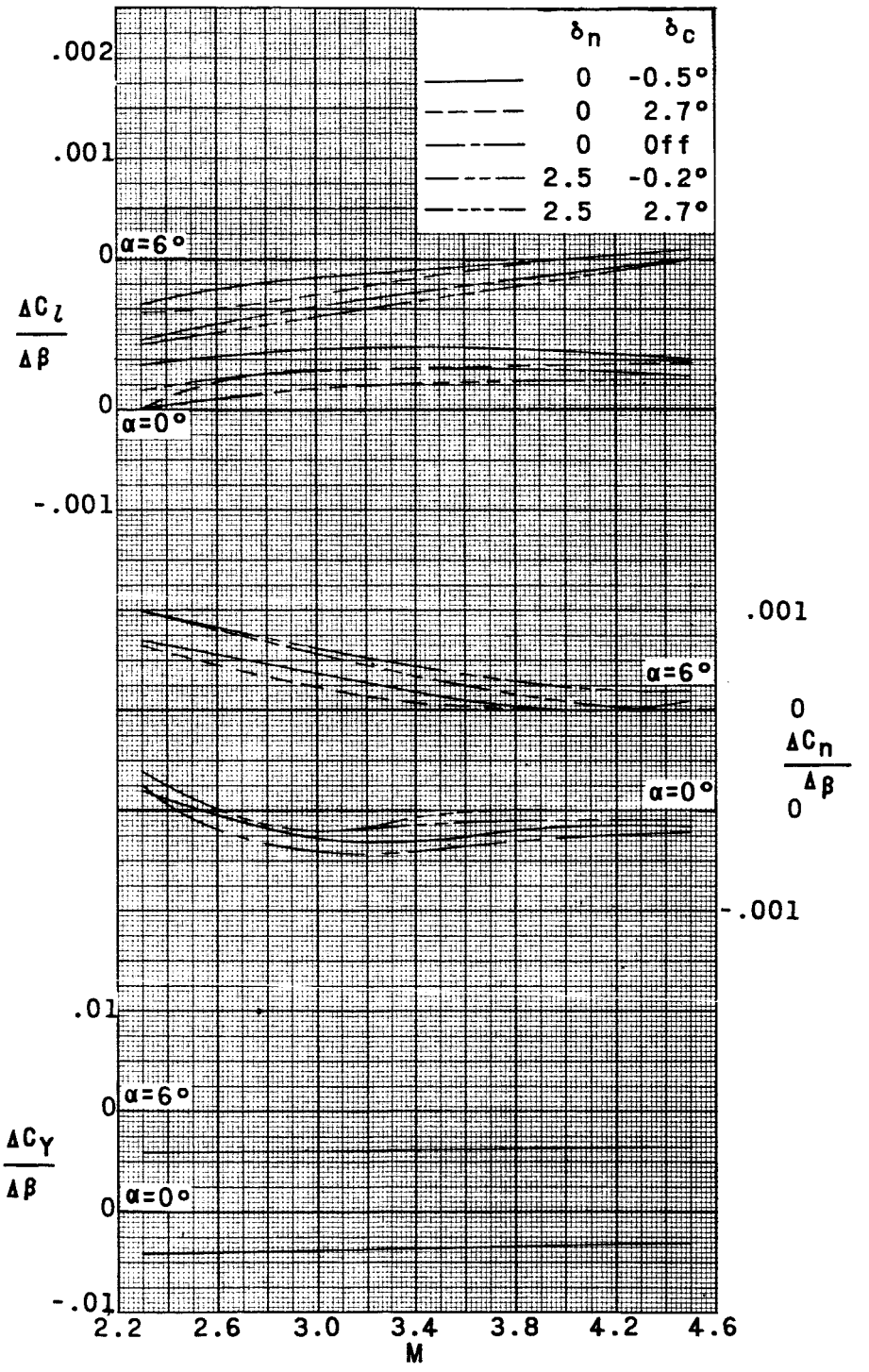

Figure 14.- Summary of lateral characteristics.

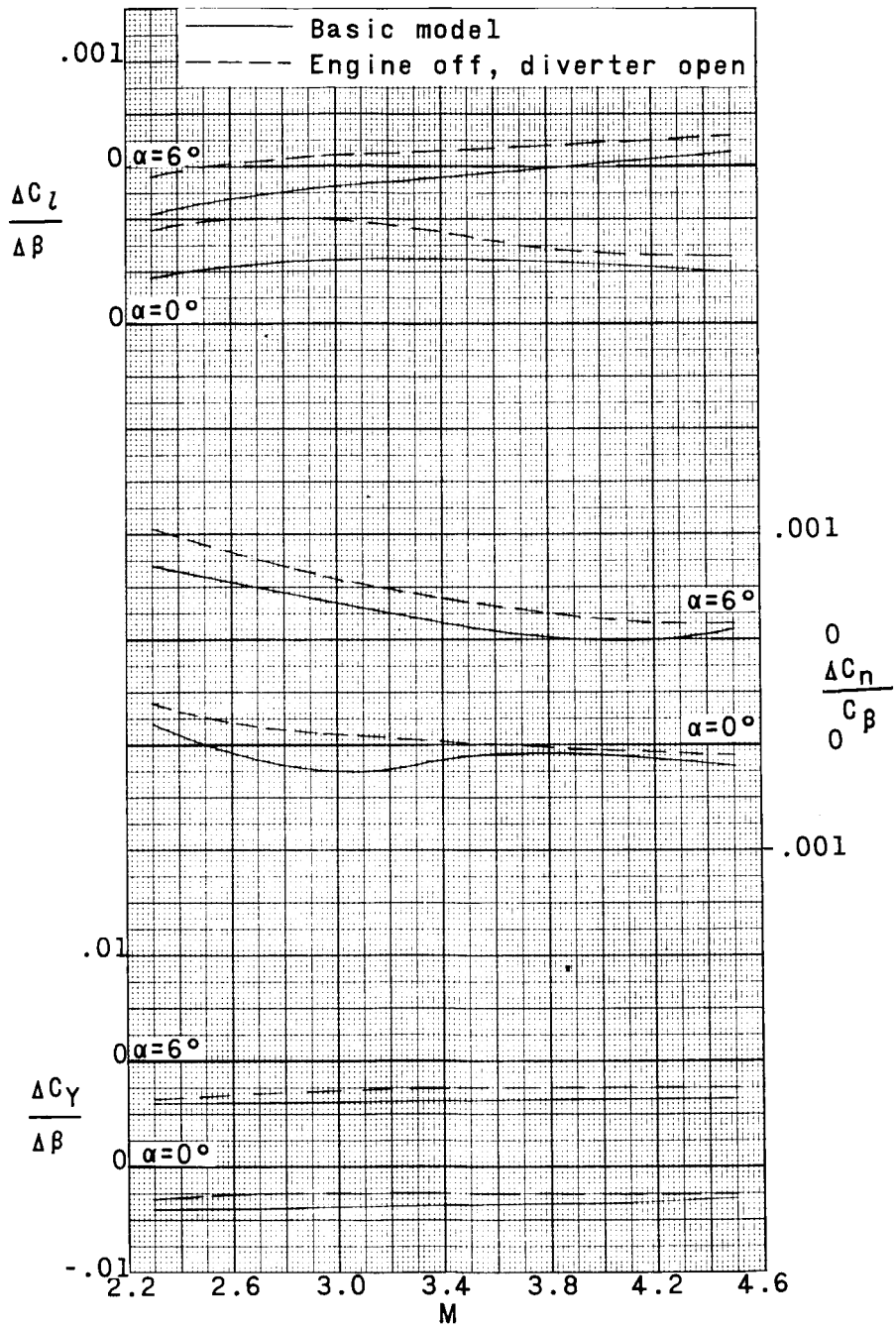

Figure 14.- Concluded.

ERRATA

NASA Technical Memorandum TM X-216

By Ausley B. Carraway, Donald T. Gregory,
and Melvin M. Carmel
March 1960

Page 12: In table I, the indicated quantities should be corrected as follows:

Wing area, sq ft	1.854
Wing aspect ratio	0.874
Canard span, in.	7.886
Canard aspect ratio	2.37

NASA - Langley Field, Va.

Issued 7-26-61